J Mater Sci: Mater Electron (2016) 27:1888–1896
DOI 10.1007/s10854-015-3969-0

CrossMark

Investigation of physical properties and impedance spectroscopy study of Cu_3SbS_3 thin films

K. Nefzi[1,2,3] · A. Rabhi[1,3] · M. Kanzari[1,2,3]

Received: 2 June 2015 / Accepted: 25 October 2015 / Published online: 31 October 2015
© Springer Science+Business Media New York 2015

Abstract Cu_3SbS_3 ingot material was successfully grown by direct melting of the constituent elements taken in stoichiometry compositions using high-purity copper, antimony and sulfide elements. Cu_3SbS_3 thin films were prepared by single source vacuum thermal evaporation method under vacuum (10^{-5} Torr) onto no heated glass substrates. The X-ray diffraction experimental data revealed that the Cu_3SbS_3 powder exhibiting an orthorhombic structure and lattice parameters a, b and c were calculated. It has been shown that the as-deposited Cu_3SbS_3 thin films were overall amorphous and the film thicknesses were around 400 nm. The absorption spectra of the films showed that the Cu_3SbS_3 compound is a direct band gap material and the gap value is closed to 1.46 eV. The as-deposited Cu_3SbS_3 films show absorption coefficients of about 2×10^5 cm^{-1} near the absorption edge. The as-deposited Cu_3SbS_3 films exhibit p-conductivity type by using hot probe method. A Schottky diode (Al/p-Cu_3SbS_3/Mo) was fabricated by simple deposition of pure Aluminum on the front side of the Cu_3SbS_3 thin film. I–V characteristics show that the Al makes Schottky contact with p-Cu_3SbS_3. Impedance spectroscopy technique was used to evaluate the conduction processes of the samples as a function of temperature (598–673 K) in the range 1 Hz–13 MHz. We found a decrease with temperature of the entire serial resistance R_s, the parallel resistance R_p and the capacitance C_p. In effort to modeling these results an equivalent electrical circuit was used. From the Arrhenius diagram, we estimated activation energy at 0.16 eV which represents the energy difference between the trap level and the valence band.

✉ K. Nefzi
khaoulanefzi88@gmail.com

1 Ecole Nationale d'Ingénieurs de Tunis Laboratoire de Photovoltaïque et Matériaux Semi-conducteurs (LPMS), Université de Tunis El Manar (UTM), BP 37 le Belvédère, 1002 Tunis, Tunisia

2 Département de Physique, Faculté des Sciences de Bizerte, 7021 Jarzouna, Bizerte, Tunisia

3 Université de Tunis, IPEITunis Montfleury, Tunis, Tunisia

1 Introduction

Copper antimony sulfide materials have attracted researchers because they are cheap, readily available. The Cu–Sb–S compounds are composed of low-toxicity and abundant elements [1]. These properties make these materials attractive candidates for many device applications. Cu_3SbS_3 is one member of this family. It has the advantage of a nearly ideal band gap for solar photo conversion with a direct band gap of 1.5 eV [2]. It is a p-type semiconductor and has a high absorption coefficient with value up to 10^5 cm^{-1} [2, 3]. All these properties make Cu_3SbS_3 an attractive candidate for a variety of applications in the fields of thermoelectric and photovoltaic [3, 4]. Many methods were used to elaborate this material. For example, Cu_3SbS_3 powder have synthesized by solution-based method [2], by solvothermal route [5] and Cu_3SbS_3 thin films have deposited by sputtering [6].

The Schottky junction is one of the fundamental structures in electronics and finds application in electronic devices such solar cells, light detectors and integrated circuits [7–9]. However, the performance and the reliability of a Schottky diode are considerably influenced by the quality of the interface between the deposited metal and the contact surface of the semiconductor [10]. So, in this work, we present results concerning the elaboration of the

Cu_3SbS_3 thin films made by single source vacuum thermal evaporation method. The characterizations of the structural, electrical, and optical properties of the Cu_3SbS_3 thin film have been studied. We present and at our knowledge for the first time the Schottky junction (Al/p-Cu_3SbS_3/Mo) completely elaborated by vacuum thermal evaporation method. We investigated the dominant current transport conduction mechanisms. Based on current–voltage and capacitance–voltage characteristics, we calculated the junction parameters, such as barrier height, ideality factor, serial resistance, and saturation current. The temperature dependence of the impedance measurements was analyzed in order to understand the effects of interface and the thermionic emission mechanism on this Schottky junction.

2 Experimental procedures

2.1 Synthesis of Cu_3SbS_3 powder

The compound Cu_3SbS_3 was synthesized by direct fusion of the component elements weighted in the stoichiometric proportions 3:1:3 [11]. High purity Cu, Sb and S chemical elements in solid state (99.999 %) were sealed in vacuum (10^{-5} Torr) in a quartz ampoule. The sealed quartz ampoule was placed into horizontal position in programmable furnace (type Nabertherm-Germany). For the synthesis, the temperature of the furnace was increased from room temperature to 600 °C with a slow rate of 20 °C/h in order to avoid explosions due to sulfur vapor pressure (2 atm at 493 °C and 10 atm at 640 °C). The temperature was kept constant to 600 °C for 24 h. Then, the temperature was increased with rate of 26 °C/h up to 1000 °C. A complete homogenization could be obtained by keeping the melt at 1000 °C for 48 h. After that, the temperature was lowered to 800 °C at a rate of 10 °C/h and the furnace was cooled to room temperature (see Fig. 1). Then, the ampoule was removed from furnace and was broken to retrieve the synthesized ingot. The ingot is homogeneous and bright gray in color (Fig. 2). X-ray diffraction (XRD) of powder showed that only homogenous Cu_3SbS_3 phase was present in the ingot. Crushed powder of this ingot was used as raw material for the film preparation by vacuum thermal evaporation.

2.2 Film preparation

Thin films of Cu_3SbS_3 were deposited onto no heated well-cleaned glass slides substrates (Corning 7059) by single source vacuum thermal evaporation method under vacuum of 10^{-5} Torr. These glass substrates were cleaned with hydrochloric acid, the ultrasonic device, detergent, deionized water, then with acetone. Tungsten boat was used as an evaporation source. The material ($\sim$0.15 g) was placed into the tungsten boat with a uniform distribution in order to prevent its ejection during the evaporation. The substrates were placed at 15 cm above the source, so that their surfaces are perpendicular to the vapor flux. Typical as-deposited films thicknesses were in the range (350–400 nm). The films prepared by this method were subjected to different characterization techniques.

2.3 Schottky junction fabrication

The p-type semiconductor Cu_3SbS_3 is used as an active material. A layer of Molybdenum with thickness 700 nm deposited previously by sputtering on a glass is used as a substrate. Then the p-Cu_3SbS_3 thin film of 400 nm thickness is deposited on the Molybdenum using vacuum thermal evaporation. Aluminum (Al) was used as a top electrode on p-Cu_3SbS_3 layer. The schematic diagram of the fabricated device (Al/p-Cu_3SbS_3/Mo) is shown in Fig. 3.

2.4 Characterization

The structural properties of the powder and the prepared film were examined using Philips X'Pert X-ray diffractometer with a monochromatic CuK_α radiation ($\lambda = 1.5406$ Å and 40 kV, 30 mA). Optical transmittance (T) and reflectance (R) were measured at normal incidence in the wavelength range 300–1800 nm using a Shimadzu UV–visible–NIR spectrophotometer. Film thickness was measured by interference fringes method [12]. The absorption coefficient was deduced from transmittance and reflectance spectra. The type of conductivity of the Cu_3SbS_3 material was determined by the hot probe method measurement [13].

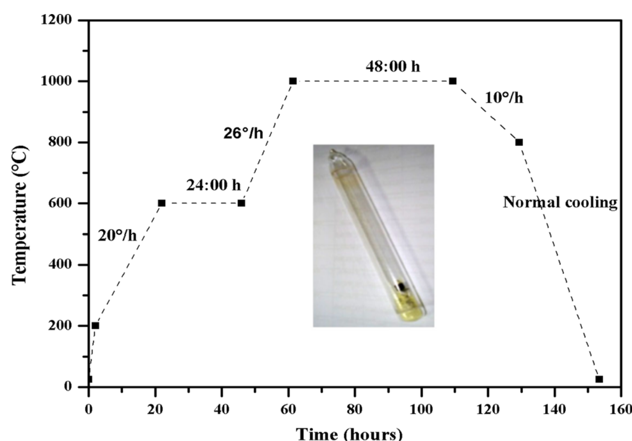

Fig. 1 Schematic of the temperature profile and the shape of the growth ampoule

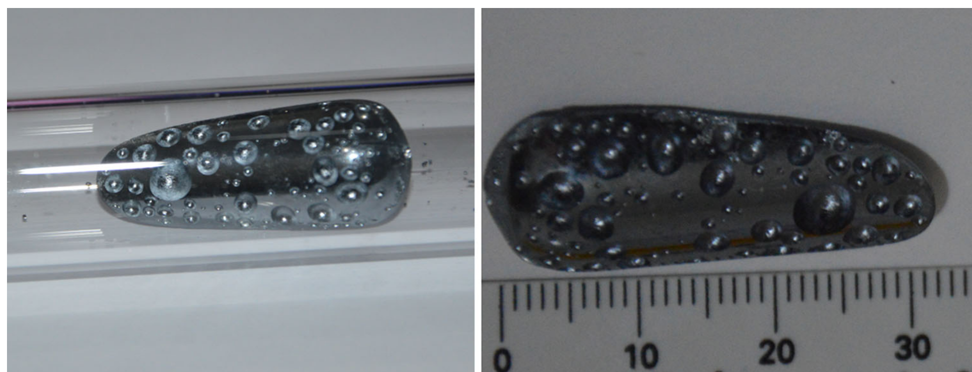

Fig. 2 Photography showing the Cu_3SbS_3 ingot

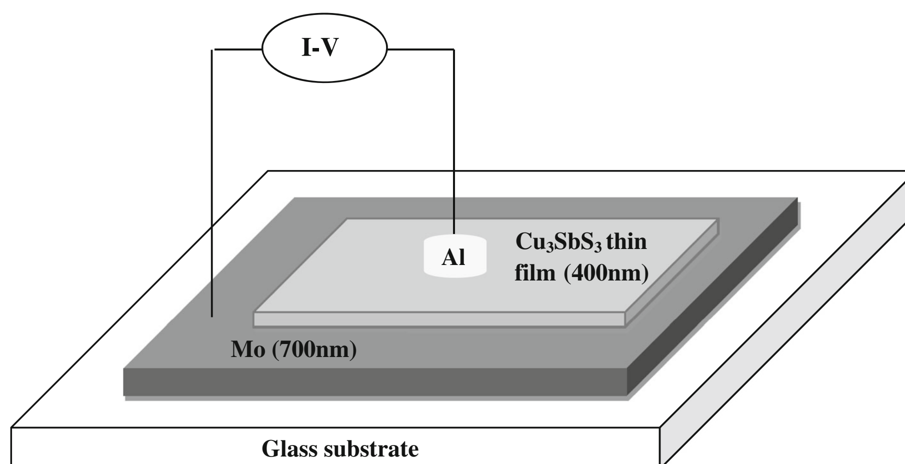

Fig. 3 The structure of (Al/p-Cu_3SbS_3/Mo) Schottky junction

The current–voltage (I–V) characteristic of (Al/p-Cu_3SbS_3/Mo) Schottky junction has been performed with Agilent N6762A and the capacitance voltage (C–V) measurement was also performed at room temperature using a low frequency impedance analyzer (HP 4192A) at a frequency of 80 kHz. Finally, the electrical measurements of real and imaginary components of impedance parameters (Z' and Z'') were made over a wide range of temperature (598–673 K) and frequency (1 Hz–13 MHz) by means of Hewlett-Packard HP 4192 impedance analyzer.

3 Results and discussion

3.1 Structural properties of powder

Figure 4 shows the X-ray diffraction (XRD) pattern of a Cu_3SbS_3 powder, which suggests that the material is single-phase, crystallized in the orthorhombic structure with a Pbam (55) space group (JCPDS 024-1289). The sharp peaks in the XRD pattern indicate good crystallinity of the synthesized material. The absence of any additional peaks confirms the phase purity of the synthesized Cu_3SbS_3 material. The lattice parameters a, b and c of Cu_3SbS_3 were calculated by using this equation [14]:

$$\frac{1}{d^2} = \frac{h^2}{a^2} + \frac{k^2}{b^2} + \frac{l^2}{c^2} \tag{1}$$

where d is interplanar spacing determined using Bragg's equation and h, k, l are the miller indices of the lattice planes. We found 10.2471, 13.2526 and 7.8463 Å corresponding to the lattice parameters a, b and c values respectively. This result is in good agreement with other studies [4].

The size of the crystallites calculated from the Debye–Scherrer formula [15] using the preferential direction along (321) plane at $2\theta = 31.624°$ is 68 nm.

3.2 Structural properties of Cu_3SbS_3 thin film

The Cu_3SbS_3 thin film prepared under optimum conditions on glass substrate was physically stable and had very good adhesion to the substrate. The X-ray diffraction pattern corresponding to the Cu_3SbS_3 thin film is shown in Fig. 5.

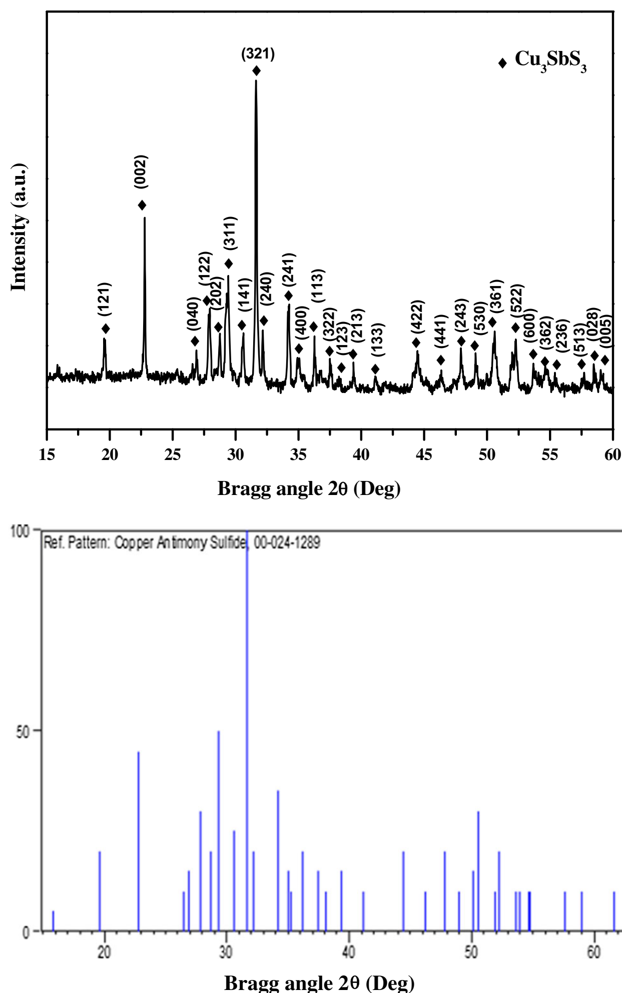

Fig. 4 X-ray diffraction pattern of Cu_3SbS_3 powder

It is clear that the as-deposited film is overall amorphous with presence of very lower peaks and probably attributed to the β-Cu_3SbS_3 phase (JCPDS 82-0851). In fact, this overall amorphous nature of the film formed at low substrate temperature is due to the non-availability of sufficient thermal energy for the diffusion of adatoms on the substrate surface for the nucleation [16].

3.3 Optical properties of Cu_3SbS_3 thin film

The investigation of optical properties of the deposited thin films is one of the most useful tools for understanding the optical absorption mechanisms in both crystalline and amorphous materials. Therefore, for the Cu_3SbS_3 thin film, the transmittance (T) and reflectance (R) spectra were recorded in the spectral range 300–1800 nm. This range covers the fundamental optical absorption edge and the transition regions of the semiconductor materials. The obtained spectra are shown in Fig. 6. The transmittance and the reflectance spectra show interference patterns with sharp fall of the transmission at the band edge, which is an indication of good homogeneity of the film [17].

From the spectral data the absorption coefficient, α, was calculated using the relationship [18]:

$$\alpha = \frac{1}{d} \mathrm{Ln} \left[\frac{(1 - R)^2}{T} \right] \quad (2)$$

where d is the film thickness. Figure 7 shows the absorption coefficient α versus the photon energy hν for the as-deposited Cu_3SbS_3 thin film. We noted a high absorption coefficient of about 2×10^5 cm^{-1} in the visible and the near-IR spectral range.

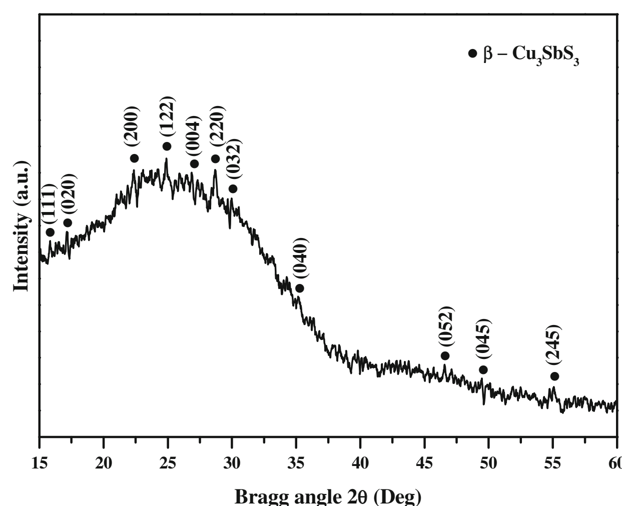

Fig. 5 X-ray diffraction pattern of Cu_3SbS_3 thin film as-deposited

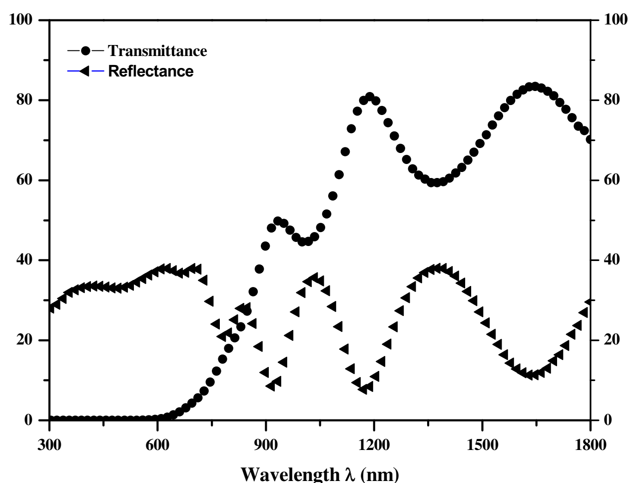

Fig. 6 Optical reflectance and transmittance of Cu_3SbS_3 thin film

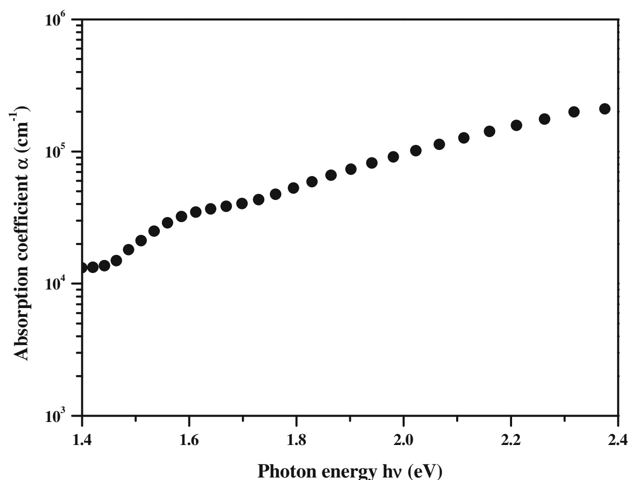

Fig. 7 Absorption coefficient spectra of Cu_3SbS_3 thin film as-deposited

For optical applications of semiconducting materials, one of the most important aspects is to determine the range of the wavelength covering the energies of the gaps between the valence and conduction band extreme because it gives the useful information about the region transparency for the film material [19]. In the crystalline and amorphous materials, the optical absorption dependence of the photon energy is expressed by the following relationship [20]:

$$\alpha h\nu = A(h\nu - E_g)^n \tag{3}$$

where A is constant, E_g is the optical band gap and the exponent n is a number that characterizes the optical absorption process and is theoretically equal to 1/2, 2, 1/3 or 2/3 for indirect allowed, direct allowed, indirect forbidden and direct forbidden transitions, respectively [21, 22]. It is well known that Cu_3SbS_3 material is a direct gap semiconductor with a band gap of about 1.5 eV [2]. The extrapolation of the linear part of $(\alpha h\nu)^2$ with the energy axis in y-intercept reveals a direct band gap value of 1.46 eV (see Fig. 8).

The band gap value and direct absorption nature of Cu_3SbS_3 phase make this material as an attractive candidate for solar energy conversion and opto-electronic applications [2, 3].

3.4 Electrical properties

Various methods are used to determine Schottky barrier parameters; these include current voltage (I–V) analysis, capacitance–voltage (C–V) analysis, photoelectron spectroscopy, activation energy method, … [23]. I–V analysis method is the simplest of all methods since it involves direct measurement of current voltage and provides first-hand information about the nature of the developed barriers across the interface.

The theoretical current–voltage characteristic of the junction diode is given by the following known relationship [24]:

$$I = I_0\left[\frac{q}{nkT}(V - R_s I) - 1\right] \tag{4}$$

where I_0 the reverse saturation current, q is the electronic charge, k the Boltzmann constant, T the absolute temperature in Kelvin, V the applied voltage, R_s the serial resistance and n the ideality factor.

Experimentally, the current–voltage characteristic studied under forward and reverse bias conditions of the (Al/p-Cu_3SbS_3/Mo) junction at room temperature is shown in Fig. 9. The rectifying behavior confirms that this junction acts like a Schottky diode.

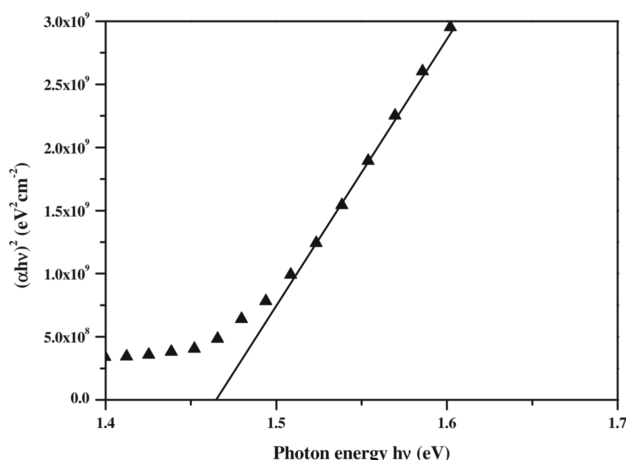

Fig. 8 Plot of $(\alpha h\nu)^2$ versus hν for the Cu_3SbS_3 thin film as-deposited

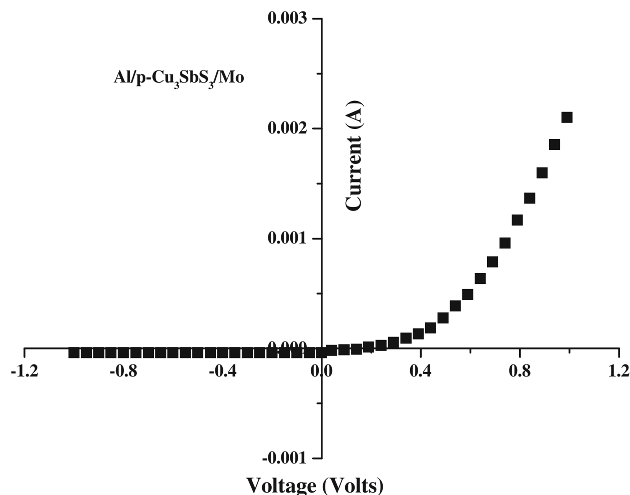

Fig. 9 Experimental current–voltage characteristic of Al/p-Cu_3SbS_3/Mo Schottky junction at room temperature

The approximated Eq. (1) up to the threshold potential can be written in the following logarithmic form [24]:

$$\mathrm{Ln(I) = Ln(I_0) + \frac{q}{nkT}(V - R_sI)} \tag{5}$$

I_0 is the reserve current saturation derived from the straight line intercept of Ln (I) at V = 0 (see Fig. 10), estimated to be 1.34 μA.

The value of the ideality factor n and serial resistance R_s can be determined from the following functions using the following equation [24]:

$$\mathrm{\frac{dV}{dLn(I)} = R_sI + \frac{nkT}{q}} \tag{6}$$

Figure 11 shows the variation of $\frac{dV}{dLn(I)}$ versus the current density I. It has, in fact, a linear behavior and we can easily extract both R_s and n which are estimated to be 47 Ω and 1.53 respectively.

The capacitance measurements were performed at room temperature at a frequency of 80 kHz under applied forward and reverse DC bias sweeps (−4 to 4 V) with an ac oscillation level of 0.5 mV (see Fig. 12). The depletion layer capacitance C per unit area can be given by the known expression [25]:

$$\mathrm{C^{-2} = \frac{2}{q\varepsilon_s N_A}[V_0 - V]} \tag{7}$$

where, ε_s is the dielectric constant of semiconductor, V the applied voltage, N_A the carrier acceptors concentration and V_0 is the built-in potential.

The Capacitance–voltage C^{-2} – V in the reverse bias voltage, at room temperature and at 80 kHz, was studied. Is a straight line, of which the intercept with the voltage axis gives the value of the built-in potential $V_0 = 0.824$ eV.

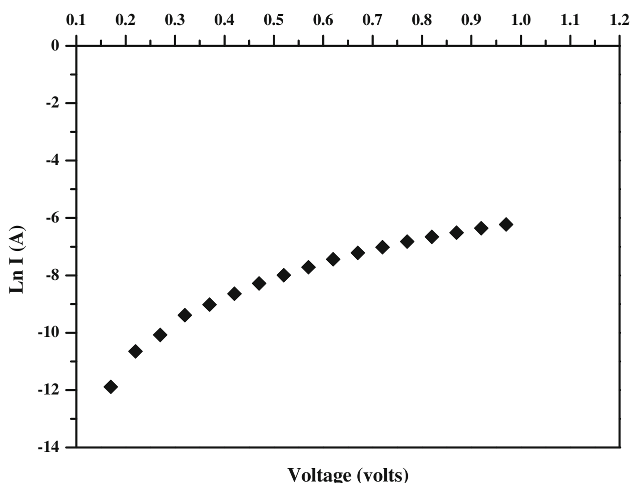

Fig. 10 The logarithm of the current density Ln(I) versus the forward bias voltage (V) of the Al/p-Cu_3SbS_3/Mo Schottky junction at room temperature

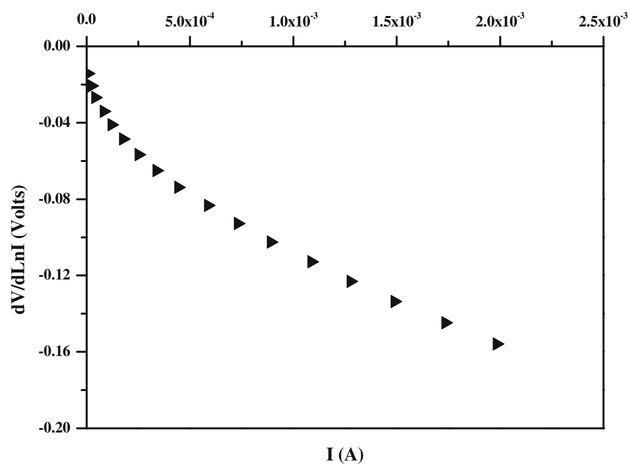

Fig. 11 $\frac{dV}{dLn\ I}$ versus the current density at room temperature for Al/p-Cu_3SbS_3/Mo Schottky junction

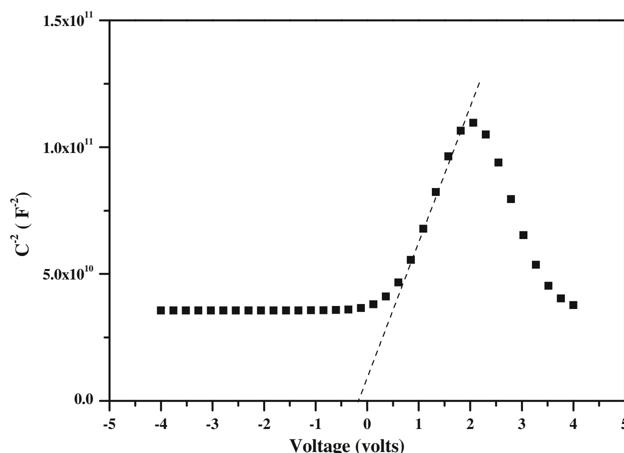

Fig. 12 C^{-2} versus Voltage at room temperature for Al/p-Cu_3SbS_3/Mo Schottky junction

The barrier height is given by the following equation [25]:

$$\varphi_b = \mathrm{V_0 + V_n} \tag{8}$$

where V_n the potential difference between the Fermi level and the top of the valence band in the Cu_3SbS_3 can be obtained by the following relationship:

$$\mathrm{V_n = \frac{kT}{q} Ln\left(\frac{N_v}{N_A}\right)} \tag{9}$$

Where N_v is effective density of states in the valence band of the Cu_3SbS_3 semiconductor. The barrier height estimated from the extrapolated intercept of C^{-2} with the voltage axis is about 0.849 eV.

Figure 13 shows the complex impedance spectra (Z″ versus Z′) obtained by plotting the imaginary part with corresponding real part for (Al/p-Cu_3SbS_3/Mo)

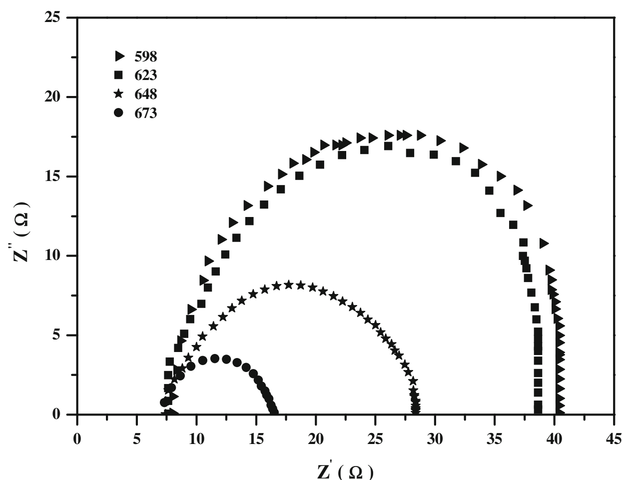

Fig. 13 Nyquist diagram of Al/p-Cu_3SbS_3/Mo heterojunction at different temperatures

heterostructure in the temperature range for (598–673 K). The electrical response can be fitted as an equivalent AC circuit composed by a single parallel resistance R_p and capacitor C_p network connected to a serial resistance R_s. The complex impedance of this electrical equivalent AC circuit with given R_s, R_p and C_p is expressed as [26]:

$$Z = R_s + \frac{1}{\frac{1}{R_p} + j\omega C_p} = Z' + jZ'' \quad (10)$$

Z' is the real part of the complex impedance and Z'' is its imaginary part. Equation (10) can be reorganized to separate real and imaginary parts:

$$Z' = R_s + \frac{R_p}{1 + \omega^2 R_p^2 C_p^2}, \quad Z'' = \frac{-\omega C_p R_p^2}{1 + \omega^2 R_p^2 C_p^2} \quad (11)$$

The values of the serial resistance R_s and the total resistance ($R_s + R_p$) were obtained from a low and high frequencies by intercepting the Z' axis respectively. The value of capacitance C_p was found to be slightly frequency dependent. The analysis of experimental data of the sample show that the semi-circles are slightly depressed and their maximum shift to higher frequencies as the temperature increases. The diameter and the maximum of the semi-circles decrease with increasing temperature.

It can be observed that all the serial resistances, the parallel resistances and the capacitance decrease with increasing temperature due probably to improvement of the junction structure. Figures 14 and 15 illustrate the evolution of the equivalent circuit parameters as a function of temperature. This observation leads to the conclusion that the electrical conductivity is thermally activated as well as the relaxation times distribution [27]. To study the relaxation time as a function of temperature, we plot Z'' versus frequency at different temperatures (see Fig. 16). We

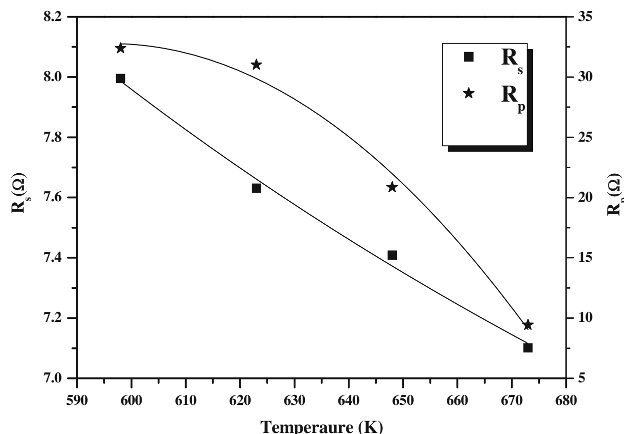

Fig. 14 Variation of the serial resistances and parallel resistances for different temperatures

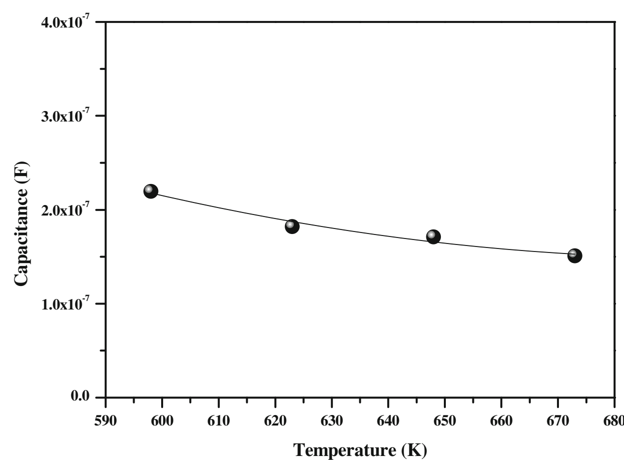

Fig. 15 The variation of capacitance versus temperature

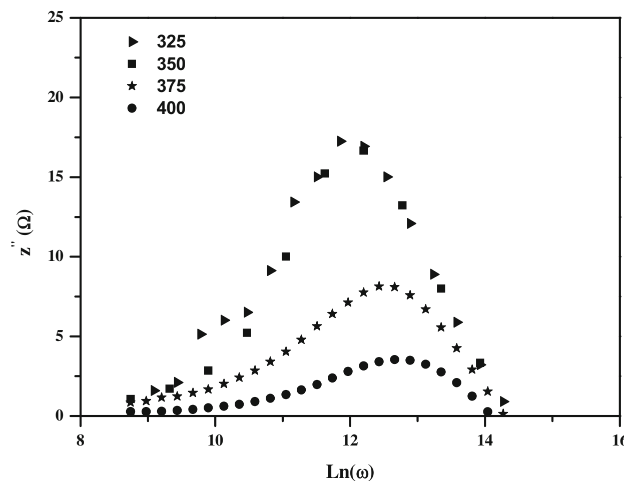

Fig. 16 Angular frequency dependence of Z'' at different temperatures

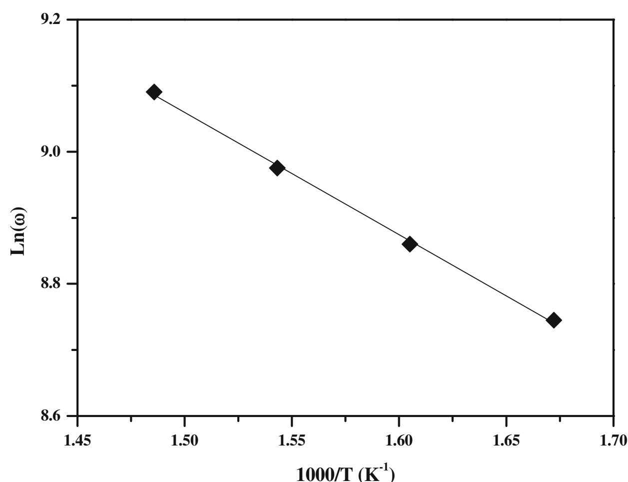

Fig. 17 Arrhenius diagram of the frequency

observed, when increasing the temperature, the frequency of the imaginary part of the impedance, shifts towards the higher frequencies. The frequency ω_m (corresponding to the maximum of imaginary part of the impedance) gives the most probable relaxation time τ_m from the condition $\omega_m \tau_m = 1$. The most probable relaxation time follows the Arrhenius law from expression [28] below:

$$\omega_m = A\nu_{th}\sigma_p N_\nu \quad (12)$$

where A is the dimensionless quantity related to the degeneracy factor of the trap and the fixed charge with the depletion region, ν_{th} is the average thermal velocity of the holes in the valence band, σ_p is the capture cross-section of the trap and E_a is the energy difference between the trap level and the valence band. As shown in Fig. 17, the expression of $\mathrm{Ln}(\omega) = f(1000/T)$ leads to a linear function, in good agreement with expression (12). The value of activation energy was estimated to 0.16 eV.

4 Conclusion

In summary, Cu_3SbS_3 material was successfully synthesized by direct melting of the constituent elements in vacuum. The XRD spectra of powder indicate the high crystallinity of the synthesized Cu_3SbS_3 material. Cu_3SbS_3 thin film has been successfully deposited on glass substrate using the vacuum thermal evaporation technique. The structural, optical and electrical properties of the as-deposited Cu_3SbS_3 thin film are studied. The absorption coefficient deduced from optical measurements is $>10^5$ cm^{-1} in the range of 1.4–2.4 eV. The direct band gap energy value to be estimated 1.46 eV. The as-deposited Cu_3SbS_3 thin film exhibits p-type conductivity.

The (Al/p-Cu_3SbS_3/Mo) junction was fabricated and studied by using I–V, C–V and impedance measurements in the range of temperature (598–673 K). The rectifying behavior confirms a Schottky junction diode with p-type absorber layer. An ideality factor of 1.58 and a serial resistance of 47 Ω were extracted from the experimental data. C–V measurement reveals that the barrier height of this heterostructure is evaluated to 0.489 eV. The complex impedance spectroscopic technique was used to characterize relaxation process in (Al/p-Cu_3SbS_3/Mo) Schottky junction diode. The impedance data show that the observed dielectric responses can be described by an electrical equivalent circuit and we found that their parameters (R_s, R_p and C_p) decrease when the annealing temperature increases. An activation energy of 0.16 eV was found. Those results are very promising for preparing thin film solar cells with p-Cu_3SbS_3 as an absorber layer.

References

1. S. Sogawa, Y. Tokai, W. Septina, T. Harada, M. Matsumura, RSC Adv. (2014). doi:10.1039/C4RA0768F
2. K. Ramasamy, H. Sims, W.H. Butler, A. Gupta, Chem. Mater. **26**(9), 2891 (2014)
3. J. van Embden, Y. Tachibana, J. Mater. Chem. **22**, 11466 (2012)
4. Aoife B. Kehoe, Douglas J. Temple, Graeme W. Watson, David O. Scanlon, Phys. Chem. Chem. Phys. **15**, 15477 (2013)
5. M.X. Wang, G.H. Yue, X.Y. Fan, P.X. Yan, J. Cryst. Growth **310**, 3062 (2008)
6. P. Maiello, G. Zoppi, I. Forbes, R. Miles, N. Pearsall, Sol. Energy Mater. Sol. Cells **113**, 186 (2013)
7. E.H. Rhoderick, R.H. Williams, *Metal-Semiconductor Contacts*, vol. 48 (Oxford University Press, Oxford, 1988), p. 20
8. S. Chand, J. Kumar, J. Appl. Phys. **82**, 5005 (1997)
9. E.H. Rhoderick, R.H. Williams, *Metal-Semiconductor Contacts*, vol. 19 (Oxford University Press, Oxford, 1988), p. 252
10. M.E. Aydin, N. Yildirim, A. Türüt, J. Appl. Phys. **102**, 043701 (2007)
11. P. Rudolph, F.M. Kiessling, Cryst. Res. Technol. **23**, 1207 (1988)
12. L. Vriens, W. Rippens, Appl. Opt. **22**, 4105 (1983)
13. A. Axelevitch, G. Golan, Electron. Energ. **26**, 187 (2013)
14. M. Ladd, R. Palmer (Plenum Publishers, New York, 2003). doi:10.1007/978-1-4615-0101-5
15. B.D. Cullity, *Elements of X-ray diffraction*, 2nd edn. (Addison-Weasley, London, 1978)
16. R. Mamazza Jr, D.L. Morel, C.S. Ferekides, Thin Solid Films **26**, 484 (2005)
17. A. Rabhi, Y. Fadhli, M. Kanzari, Vacuum **112**, 59 (2015)
18. D.E. Milovzorov, A.M. Ali, T. Inkuma, Y. Kurata, T. Suzuki, S. Hasegawa, Thin Solid Films **382**, 47 (2001)
19. N.K. Sahoo, K.V.S.R. Apparao, Appl. Phys. A **63**, 195 (1996)
20. N.F. Mott, E.A. Davis, *Electronic Processes in Non-Crystaline Materials* (Clarendon Press, Oxford, 1971)
21. K. Bindu, J. Campos, M.T.S. Nair, A. Sanchez, P.K. Nair, Semicond. Sci. Technol. **20**, 496 (2005)
22. A.F. Qasrawi, Cryst. Res. Technol. **40**, 610 (2005)
23. A.A.M. Farag, I.S. Yahia, M. Fadel, Int. J. Hydrogen Energy **34**, 4906 (2009)

24. D.K. Shroder, *Semiconductor Material and Device Characterization*, 3rd edn. (IEEE Press, Piscataway, 2006)
25. E.H. Rhoderick, R.H. Williams, *Metal–semiconductor Contacts*, 2nd edn. (Clarendon, Oxford, 1988)
26. P. Agarwal, M.E. Orazem, J. Electrochem. Soc. **142**, 4159 (1995)
27. B. Roy, S. Chakrabarty, O. Mondal, M. Pal, A. Dutta, Mater. Charact. **70**, 1 (2012)
28. C. Ostos, L. Mestres, M.L. Martínez-Sarrión, J.E. Garcia, A. Albareda, R. Perez, Solide State Sci. **11**, 1016 (2009)